

¹ Punith Kumar Y.² Dr. J. Upendar

A New Ultra-Gain Step-Up Converter with Continuous Input Current for Micro-Grid Applications



Abstract: - For green energy micro-grid applications, it is crucial to have a step-up converter that can produce a wide range of voltages. This converter is necessary to match the low voltage output of the micro-grid with the DC-bus voltage and must have continuous input current. A new ultra-gain step-up converter with continuous input current, is proposed to achieve this objective. The proposed converter is a non-coupled inductor-based, non-isolated boost converter with continuous input current which is suitable to operate at a high voltage suitable for green energy based micro-grid applications. The proposed DC-DC configuration yields in increased efficiency, ultra-voltage gain with less duty ratios, minimal voltage stresses on the switches, and a high boost capacity. This converter has been designed and provided the detailed theoretical analysis and comprehensive method to obtain high gain. The simulation results show that the efficiency is 97.9% with ripple factor of 0.5. Additionally, this converter is tested under different duty ratios and the results are presented. The proposed system is unique because of its design and increased efficiency, which enable larger output voltages and a more significant gain for sustainable energy systems. Finally, the comparative study is also presented to show the competitiveness with other recent topologies.

Keywords: Microgrid, Step-Up Converter, Duty Ratio, Ripple Factor, Voltage Gain, Voltage Stress.

I. INTRODUCTION

The need for power is increasing to the point where the IEA predicts that, compared to the growth rate in 2022, the worldwide electricity demand will increase by 3% year between 2023 and 2025. Advanced economies are looking to generate more electricity while lowering the need for fossil fuels. Through the backing of policies in over 130 countries, about 3700 GW of additional renewable power is expected to come online between 2023 and 2028. According to the International Energy Agency, the proportion of renewable energy in the worldwide power generation mix is expected to increase from 29% to 35% by 2025. Promising developments have been observed recently that 2022 set a record for the yearly capacity additions of renewable electricity, totaling over 340 GW. A revolution in power electronic systems has resulted from the increased use of renewable energy sources with power converters called DC-DC converters, as the essential part that control and optimize the flow of electricity between the input system and the grid or batteries. Generation processing applications such as wind generation, solar systems, electric vehicles, microgrid, and DC distribution systems require these converters. Furthermore, power converters are essential for resolving problems with power quality in systems that are connected to the grid, particularly as renewable energy sources become more widely used. Researchers worldwide are actively pursuing the goal of installing a greater amount of renewable energy capacity in the next five years than what has been put up to this point. Only solar photovoltaics and wind energy are currently projected to achieve the Net Zero Emissions by 2050 (NZE) Scenario, making them the sole renewable energy technologies on pace to fulfil this goal.

In this paper, the proposed converter uses solar and wind energy as its input. The solar portion's output is obtained during sunshine and is dependent upon the amount of incoming solar energy. Conversely, the wind turbine's output is contingent upon the wind speed at the installation site and can be achieved at any time of day or night when the wind speed exceeds a certain threshold. In rural and isolated locations with electricity supplied by standalone units or mini-grid connections, PV/WT systems are thought to be appropriate. Steady and reliable power production can be obtained by hybridizing sources, which lowers the possibility of power outages during low-wind or low-sun periods. Hybrid systems that store energy can stabilize the grid by supplying power during times of high demand, which in turn reduces congestion and improves overall stability. More broadly, integrating wind and solar energy necessitates coordinated policy initiatives, including feed-in costs specifically intended at hybrid

¹ *Research Scholar, Dept. of Electrical Engineering, University College of Engineering, Osmania University, Hyderabad, Telangana. India.

² Asst. Professor, Dept. of Electrical Engineering, University College of Engineering, Osmania University, Hyderabad, Telangana, India.

¹Corresponding Author Email: kumar273bi@gmail.com.

structures. Mandate response techniques adjust the contributions from wind and solar energies based on simultaneous consumption designs, ensuring a balance between supply and demand [1].

For the utilization of these hybrid combinations there is a need of DC-DC converters. A number of DC-DC converters both isolated, non-isolated are examined with an emphasis on their high voltage gain, reduced switching losses, decreased voltage, and enhanced efficiency. [2] proposed an effective DC-DC converter in which voltage multiplier cells are used to produce high voltage gain and switched inductor cells are used to obtain continuous source current. Directs at a duty ratio of 27.3%, yielding a voltage gain of 10, while an 80% duty ratio yields a voltage gain of 39. In applications where the input voltage must be greatly increased to match the intended output voltage, high-gain dc-dc is frequently preferred. It is possible that a high-gain converter can be designed with fewer components to preserve cost-effectiveness and dependability. A non-auxiliary switch DC-DC boost converter with voltage gain interleaved is suggested in [3]. The intended design achieves step-up features without the need for a switched inductor/switched capacitor, a transformer, voltage multiplier cell, or connected inductor. Because there are no components present, the converter can achieve its maximum voltage gain, while the input current ripple may be larger. However, voltage multiplier cells are used in the High gain DC-DC converter to produce high voltage gain, while switching inductor cells provide the constant source current.

An analysis of several converters led to the proposal of "A high gain boost converter," which would increase the low voltage to a higher level, allowing for grid integration or powering an isolated load. High gain DC-DC converters typically use cascade at connections to increase the converters' overall gain. They also draw continuous input current, which makes them a desirable option for renewable energy applications. Boost cells, switched capacitors, switched inductors, and couple inductors are typical uses for the converters. Comparing it to other converters, its gain ratio is higher.

A Literature Survey

The article suggests a quadratic DC-DC boost converter that uses a switched-capacitor cell design to generate an extremely high voltage gain. By generating a significant voltage gain effect at a low duty cycle—thereby minimizing voltage stress on semiconductor switches, diodes, and capacitors—the converter achieved ultra-high output voltage gain without utilizing a voltage doubler circuit. Applications involving renewable energy make use of both CSC and the input-to-output side ground-sharing property. Results showed that the suggested converter [4] achieved an efficiency of 90% while generating approximately 80 W of power using a 150 W prototype; the report also covered power loss calculations, steady-state performance, and comparisons with other topologies. Results from both experiments and simulations corroborated those from the theoretical study, proving that the converter under consideration is a practical option for use in solar power applications due to its high voltage gain. The article explains a two-switch boost converter (TSBC), which adds another set of switch-diodes to the CBC circuit through a cascade effect. As a result, the gain voltage and DoFoC are enhanced. [5] Much research on power converters was prompted by the need for reliable and efficient power conversion. The mathematically predicted properties of TSBC are validated, theoretically, by both simulations and real findings. An increase in voltage gains of 3.2 to 4.3 is achieved at a duty ratio of 0.7 for the present CBC switch when the duty ratio of the extra TSBC switch is increased from 0 to 0.1. Maintaining a consistent ripple ratio, output voltage, and inductor current all lead to an increased DoFoC. The suggested converter can simply substitute the widely used CBC by cascading a pair of switch-diodes at the input side of the CBC, increasing the gain and DoFoC.

In [6], the authors introduce a DC-DC boost converter that uses switched-inductor and switched-capacitor cells to achieve high gain with a single switch. A single switch simplifies the control circuit and maintains a constant DC voltage at the output side of the suggested boost converter, even when input voltages or loads are changed. When thinking about the SC-cell in relation to the SL layout, you get a lot of efficiency. In addition to a detailed mathematical study for both continuous (CCM) and discontinuous (DCM) conduction modes, a 200 W laboratory-scale prototype is also shown. The outcomes of the hardware tests corroborate the precision of the results obtained from the theoretical study and simulation.

A new non-isolated DC-DC converter with a single switch is suggested in this article; it has great voltage gain and less stress on the semiconductors. The incorporation of a self-lift Sepic converter inside the converter allows for high voltage gain with less switch duty-cycle. Further, the input side of the converter reached "near zero" ripple current, which will prolong the stack's life in the fuel cell. Experimental results of a 100 W/240 V_{dc} output with a

24 V_{dc} input voltage are provided in order to evaluate the efficacy of the suggested method, which is based on the theoretical and practical principles described in [7]. Using the mean model as a starting point, we investigate how the proposed converter handles variations in input voltage and load current. The suggested converter's design and high efficiency make it a viable alternative for renewable energy systems and other real-world applications that demand a high voltage transfer gain.

For renewable energy systems, this study suggests a [8]. While increasing the relatively low voltage produced by solar PV panels, the suggested converter can sustainably draw input current thanks to its high voltage gain, hence reducing voltage stress on the devices. The suggested converter does not provide the highest voltage gain when compared to existing dc-dc converters. Considerations for design, boundary and discontinuous conduction modes, continuous conduction mode, and the non-ideality of the converter are all thoroughly examined. The converter's functionality is tested by creating a model in a controlled environment. The output powers of the converter are evaluated at 50–150 W with a 50% duty cycle and an input voltage of 20 V. The proposed converter achieves a 96% efficiency rate while providing a constant input current and stepping up the 20 V to 200 V while the output load consumes 100 W.

This study [9] introduces a novel energy converter for sustainable power called an isolated two-switch boosting resonant switching capacitor (ITBRSC). The ITBRSC converter offers excellent isolation when used in conjunction with a transformer and can be used in a wide range of applications with variable input voltages. Potentially, it might function as an isolated power source with a high gain for use in renewable energy systems, such as wind and electric vehicles. For the purpose of testing, we construct an ITBRSC converter with an output power of 500W. The ITBRSC converter is tested and demonstrated through experiments and simulations. The suggested isolated SC converter has a workable design and good performance, according to the results of the tests and simulations.

[10] With quadratic voltage gain and reduced voltage stress across switching components, this work presented a unique, high-gain DC-DC converter. Results were better than those of the CBC and QBC, two competing converters. In comparison to other recently developed topologies, we examined the voltage stress across switching devices, the quantity of passive components, and the converter stress. Piecewise Linear Electrical Circuit Simulation (PLCES) was also used to do the loss analysis. Theoretical and experimental evaluations demonstrated that the converter outperformed quadratic boost and current high-gain converters with regard to voltage stress across the switch and gain. At $V_{in} = 24$ V, the converter achieved its peak efficiency of 93.7%. Powerful 200-300 W converters are well-suited for usage with renewable energy sources due to their many practical uses.

The suggested converter outperforms both high gain boost converters and the conventional quadratic boost converter in terms of voltage gain [11]. A comparison analysis was carried out based on many performance criteria after the design was compared with recently presented topologies. The results showed that the architecture satisfies the requirements for grid integration and renewable and sustainable energy storage. The converter's functionality has been tested in both dynamic and steady-state scenarios using a 150W hardware prototype [12–13]. The converter functions effectively, with an efficiency of over 91% over the input power spectrum, according to the paper's loss assessment. When the output power was 66 W, the maximum efficiency was 93.6%. The converter achieves a significant voltage gain at low duty ratios. We can achieve a gain of about twelve times with a duty ratio of 0.6 under perfect circumstances.

II. PROPOSED CONVERTER

Wherever Times is specified, Times Roman or Times New Roman may be used. If neither is available on your word processor, please use the font closest in appearance to Times. Avoid using bit-mapped fonts if possible. True-Type 1 or Open Type fonts are preferred. Please embed symbol fonts, as well, for math, etc.

The purpose of proposing a converter is depending on Technical Standardization, Interoperability, Efficiency and Convenience, Innovation and Improvement, Market Expansion, Cost Reduction. Based on these factors figure 1 depicts the diagram of a proposed ultra-gain step-up configuration. Adaptations to the input and output terminals of the high gain DC/DC power converter that incorporate the invention allow it to be connected to power sources and loads, respectively. The converter consists of storage elements they are, two Inductors (L_A and L_B), and three Capacitors (C_A , C_B , and C_C), along with Uncontrolled devices such as three Diodes (D_A , D_B , and D_C), two Switches (S_A and S_B) and a load Resistance (R). Its operation is controlled by a single PWM signal. A changing input and a constant output are possible with a PWM boost converter also it lowers the noise and harmonic distortion in the

output waveform to enhance power quality. The topology of the converter can be expanded to achieve higher gains and is distinguished by its ease of use, high voltage gain, improved efficiency, continuous input current, and fewer inductors and capacitors. The following explains the proposed converter's CCM mode of operation.

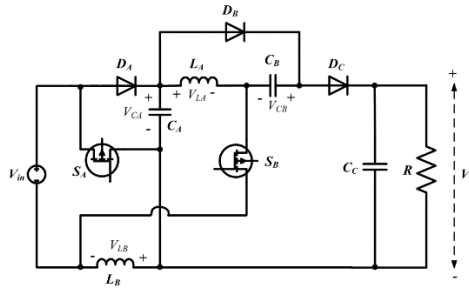


Fig 1. Proposed Ultra-Gain step-up configuration

2.1 MODE 1

In Mode 1, diodes (DA and DC) are turned off due to reverse bias while diode (DB) is turned on due to forward bias when both switches (SA and SB) are set ON. The inductor (LB) retains the magnetic energy through Vin when the switch (SA) is turned ON. The capacitor (CA) charges the inductor (LA) when the switch (SB) is turned on. A capacitor (CB) stores energy, which it releases through a diode (DB). The energy in the capacitor (CC) is released to R. Figure 2 shows the Mode-1 operation of proposed converter.

$$V_{LA} = V_{in} + V_{CA} = V_{CB} \tag{1}$$

$$V_{LB} = V_{in} \tag{2}$$

Where V_{in} = Input voltage, V_{LA} = Inductor voltage (L_A), V_{CA} = Capacitor voltage (C_A)

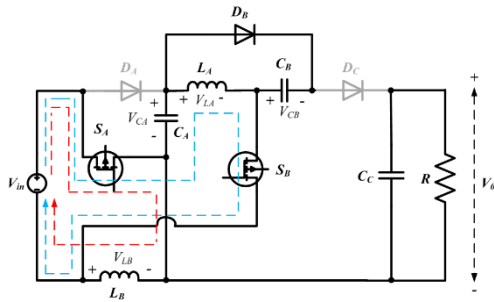


Fig 2. Mode-1: When both the active switches are conducting.

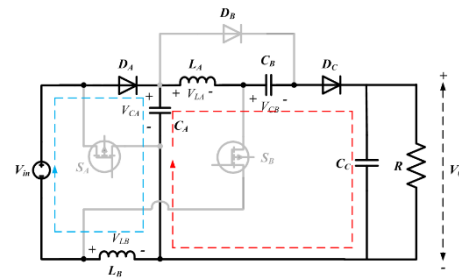


Fig 3. Mode-2: When both the active switches are not conducting.

2.2 MODE 2

In Mode 2, when the both active switches (SA & SB) are turned off, the diodes (DA and DC) are turned on by forward bias and the diode (DB) is turned off by reverse bias. The diode (DA) allows the inductor (LA) to charge the capacitor (CA). Capacitors (CC) and (LA) are charged simultaneously by the input sources, inductors (LB) and (DA), via the corresponding diodes (DC) and (DA). The converter's Mode-2 operation is shown in Figure 3.

$$V_{CA} - V_{LA} + V_{CB} - V_0 = 0 \tag{3}$$

$$-V_{LA} = V_0 - V_{CA} - V_{CB} \tag{4}$$

$$-V_{LA} = V_0 - V_{CA} - (V_{in} + V_{CA}) \tag{5}$$

$$V_{LA} = V_{in} + 2V_{CA} - V_0 \tag{6}$$

$$V_{LB} = V_{in} - V_{CA} \tag{7}$$

Where V_0 = Output voltage, V_{LB} = Inductor voltage (L_B), V_{CB} = Capacitor voltage (C_B)

2.3 Volt-Sec Balance

Inductors adhere to the volt-second balanced condition to achieve stable operation in a steady-state. If the volt-second criterion is not met, the current will steadily rise in the direction of the imbalance, potentially leading to the destruction of the inductor. Typically, when we talk about applying volt-second balancing to an inductor, it

means that the inductor is in a stable condition when the total volt-seconds over each cycle of switching are equal to zero. Now, by using volt-second principle across the inductor L_B we get,

$$V_{in}D + (V_{in} - V_{CA})(1 - D) = 0 \quad (8)$$

$$V_{CA} = \frac{V_{in}}{1-D} \quad (9)$$

Where, D is the gating pulse-width modulation (PWM) signal's duty ratio.

Now, at the inductor L_1 , apply the voltage inductor balance.

$$(V_{in} + V_{CA})D + (2V_{CA} + V_{in} - V_0)(1 - D) = 0 \quad (10)$$

$$2V_{CA} - V_{CA}D + V_{in} - V_0(1 - D) = 0 \quad (11)$$

$$V_{CA}(2 - D) - V_0(1 - D) + V_{in} = 0 \quad (12)$$

$$-V_0(1 - D) + \frac{V_{in}(2-D)}{(1-D)} + V_{in} = 0 \quad (13)$$

$$V_0(1 - D) = \frac{2V_{in} - V_{in}D + V_{in} - V_{in}D}{(1-D)} \quad (14)$$

$$V_0(1 - D) = \frac{3V_{in} - 2V_{in}D}{(1-D)} \quad (15)$$

$$\frac{V_0}{V_{in}} = \frac{(3-2D)}{(1-D)^2} \quad (16)$$

2.4 Selection of Inductors

When selecting an inductor for a DC-DC converter, several key parameters need to be considered to ensure proper operation and efficiency of the circuit. The inductance value is typically chosen based on the desired operating frequency of the converter and the amount of current ripple that can be tolerated in the circuit. Inductor with a current rating that is larger than the maximum current expected in the circuit. It is important to choose an inductor with a saturation current value more than the maximum peak current in the circuit to prevent saturation and maintain stable operation.

$$L_A \frac{dI_{LA}}{dt} = V_{in} + V_{CA} \quad (17)$$

$$L_A \frac{dI_{LA}}{dt} = V_{in} + \frac{V_{in}}{1-D} \quad (18)$$

$$L_A \frac{dI_{LA}}{dt} = \frac{V_{in} - V_{in}D + V_{in}}{1-D} \quad (19)$$

$$L_A \frac{\Delta I_{LA}}{Dt} = \frac{2V_{in} - V_{in}D}{1-D} \quad (20)$$

$$\frac{V_0}{R} L_A \geq \frac{V_{in}(2-D)DT}{1-D} \quad (21)$$

$$V_0 L_A \geq \frac{RV_{in}(2-D)DT}{1-D} \quad (22)$$

$$L_A \geq \frac{R(1-D)^2(2-D)D}{2(3-2D)f_s} \quad (23)$$

$$L_A \geq \frac{R(1-D)^4 D^2}{2f_s(3-2D)(1+D-D^2)} \quad (24)$$

$\frac{dA(t)}{dt}$ = Rate of change of inductor current (L_A) with respect to time, The load value is denoted by R , the duty ratio by D , and the switching frequency is given by f_s . L is the inductor's necessary inductance (L_A & L_B).

2.5 Selection of Capacitors

Basically, the capacitor is used for energy storage and smooth out voltage ripples in the output voltage. Considering the factors this helps in providing a more stable and continuous output voltage. The capacitor acts as a filter to reduce voltage ripple and noise in the output voltage, resulting in a cleaner and more stable output.

$$I_{CA}\Delta T = C_A\Delta V_{CA} \quad (25)$$

$$I_{CA}DT = C_A\Delta V_{CA} \quad (26)$$

$$\frac{V_0}{R(1-D)} = C_A\Delta V_{CA} \quad (27)$$

$$C_A = \frac{V_0}{R(1-D)f_s\Delta V_{CA}} \quad (28)$$

$$V_{CA} = \frac{V_{in}(3-2D)}{(1-D)^2 R(1-D)f_s\Delta V_{CA}} \quad (29)$$

$$V_{CA} = \frac{V_{in}(3-2D)}{R(1-D)^3 f_s\Delta V_{CA}} \quad (30)$$

$$C_B = \frac{V_{in}(3-2D)}{R(1-D)^2 f_s\Delta V_{CB}} \quad (31)$$

$$C_c = \frac{V_{in}(3-2D)}{R(1-D)^2 f_s \Delta V_{CC}} \quad (32)$$

III. RESULTS AND DISCUSSION

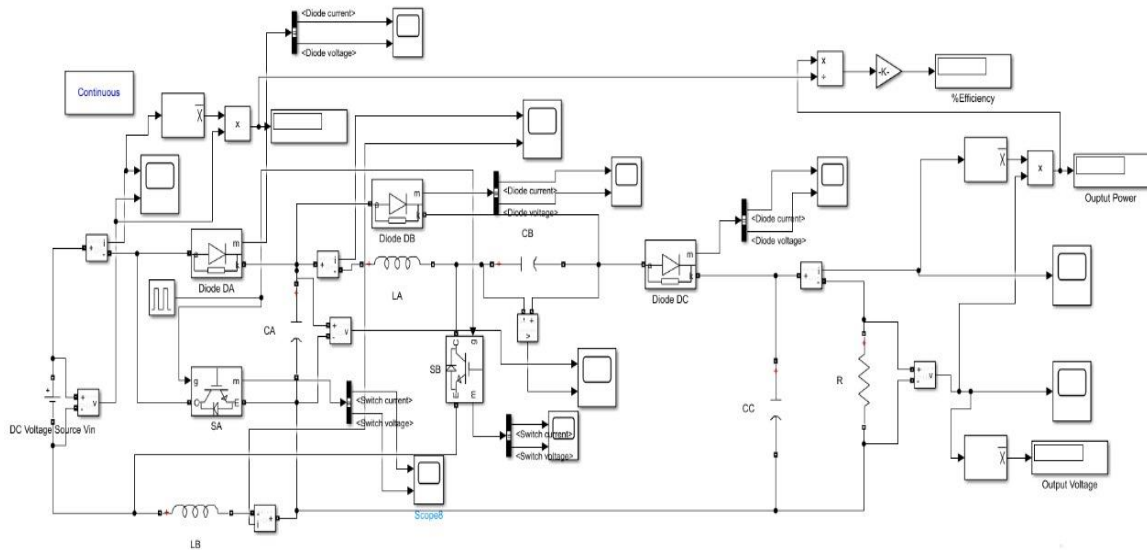


Fig 4. Simulink diagram of proposed step-up converter.

Simulink, an extension of MATLAB, is designed for modelling, simulating, and analyzing dynamic systems through block diagrams. Each block can depict a physical component, a small system, or a function. The model consists of Scopes, Mean block, gain block, Voltage and current measurement blocks fig 4 shows the Simulink diagram of proposed converter. Her a source block is used to generate input signal. The scopes are used to display the waveforms of each and every component. The measurement blocks are used to display the waveforms of the current and voltage of Inductors, capacitors and switches. Below are the parameters of each component.

TABLE 1. Parameters of proposed ultra-gain step-up converter.

PARAMETERS	SPECIFICATIONS
Input voltage	12v
Output voltage	100v
Switching Frequency	50KHZ
Inductors (L_1 L_2)	$45.8 * 10^{-6}H, 3 * 10^{-6}H$
Capacitors ($C_1 C_2 C_3$)	$164.4 * 10^{-6}F,$ $80 * 10^{-6}F,$ $80 * 10^{-6}F$
Load (R_L)	50Ω

Duty ratio	51.34
Output power	200W

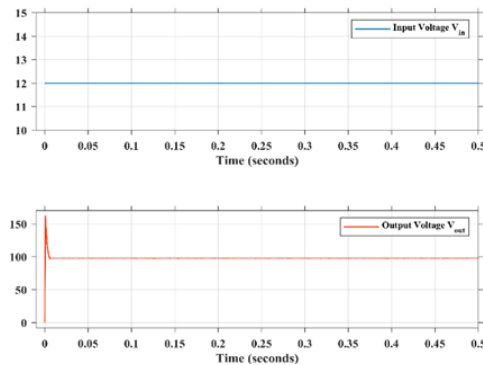


Fig 5. I/P & O/P Voltage waveforms V_{in} & V_{out}

The supply voltage the converter receives from the mains is referred to as the input, and the voltage it receives after being stepped up to the necessary voltage is referred to as the output. So, here the behavior the waveforms of input and output voltage is shown in the corresponding graphs. The 12volt input waveform and output waveform, which ranges from 0 to 97.94 volts, are interpreted in fig 5, which are colored blue and red.

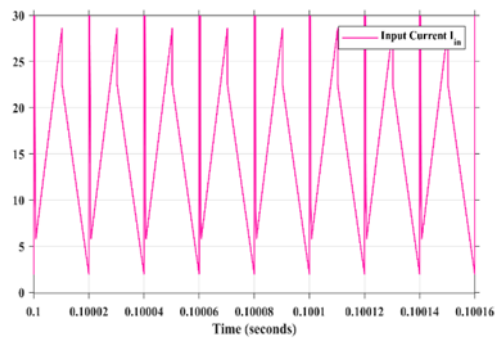


Fig 6. Input Current waveform I_{in}

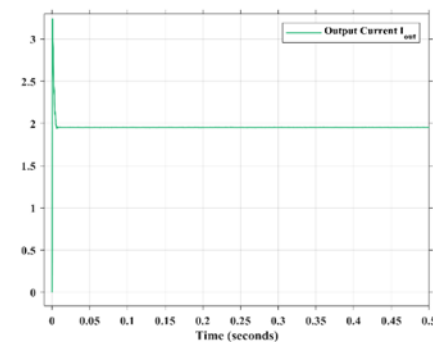


Fig 7. Output Current waveform I_{out}

The waveform of the Input and output current describes the shape of one cycle of the current. Here, the graphs display the behavior of the input and output current waveforms. In fig 6 and 7, the input waveform, which is colored pink, is 0 to 29A, while the output waveform, which is colored green, ranges from 0 to 1.95A.

The current and voltage waveforms of a switch in a DC-DC converter are crucial for analyzing the converter's performance, efficiency, and thermal behavior. They help in understanding switching losses, ensuring proper operation, and designing the converter for optimal performance and reliability. This switch acts as an intermediary device. Here, the above graphs illustrate how the switch's voltage and current waveforms behave. Graph 8 interprets the voltage waveform, which is colored yellow, and the current waveform, which is colored violet. The voltage waveform ranges from 0 to 25v and current ranges from 8 to 30A.

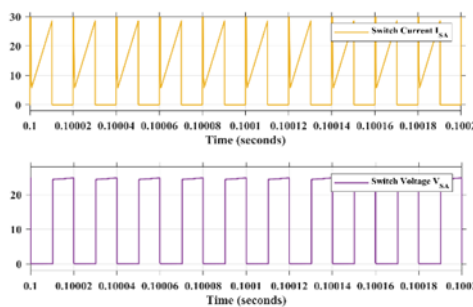


Fig 10. Voltage waveforms of Inductors L_A and L_B .

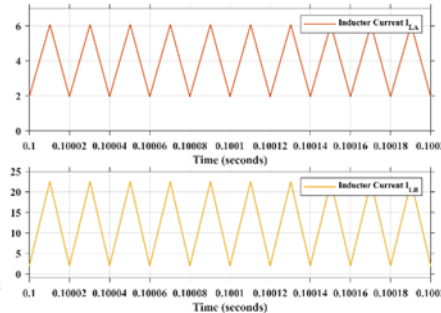


Fig 11. Current waveforms of Inductors L_A and L_B .

Voltage waveforms in an inductor of a DC-DC converter illustrate the inductor's behavior during switching cycles, including energy storage and release. They help analyze converter efficiency, switching losses, and performance, ensuring proper operation and stability of the power supply. Here, the graphs demonstrate the behavior of the voltage waveforms for L_A and L_B . Graph 10 interprets the voltage waveforms of L_A , which is -38v to 36v, and L_B , which is -12v to 13v. The waveforms are colored red and violet, respectively. When the inductor L_B retains the magnetic energy through V_{in} when the switch (S_A) and S_B are turned ON. Here, the equivalent diagrams illustrate how the current waveforms of L_A and L_B behave. The voltage waveforms of L_B , which is 2A to 22A, and L_A , which is 2A to 6A, are interpreted in Graph 11 and are represented by the colors red and yellow, respectively.

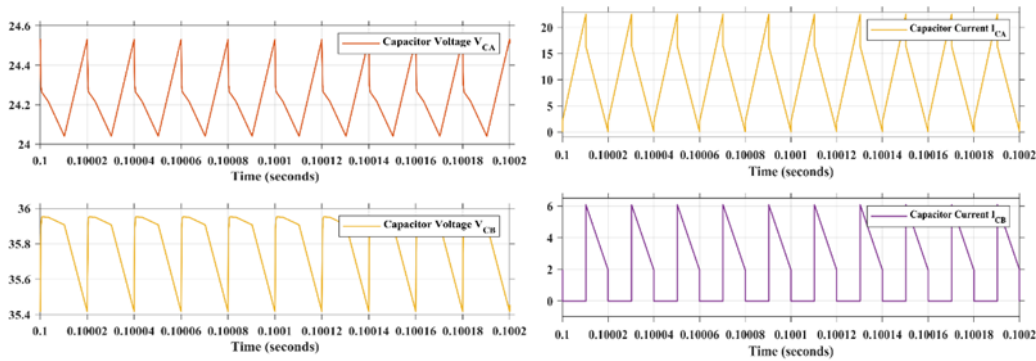


Fig 12. Voltage waveforms of Capacitors C_A and C_B . Fig 13. Current waveforms of Capacitors C_A and C_B . The solid line indicates the capacitor voltages of C_A and C_B . It is simple to see that the capacitor voltages remain well-balanced. Graph 12 interprets the voltage waveforms of C_A , which ranges from 24.1 to 24.6 volts, and C_B , which ranges from 35.5 to 36v. The color Red and yellow, depict these voltage waveforms. When switches are in the off position, these waveforms are formed. Graph 13 describes the Capacitor's (C_A) and (C_B) current waveforms, which have a range of 0 to 22.5A and 0 to 6A, respectively, are interpreted. These waveforms can be seen in the color violet and yellow.

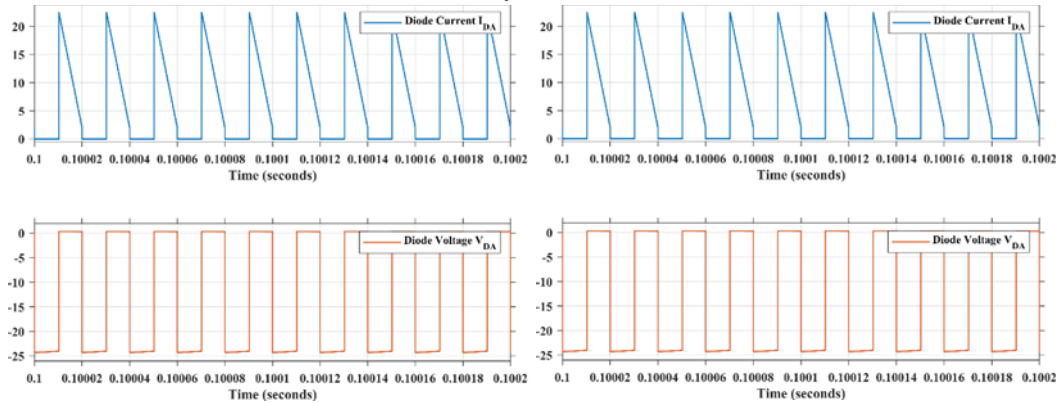


Fig 14. Voltage and Current waveforms of Diode D_A . Fig 15. Voltage and Current waveforms of Diode D_B . When the switches are deactivated. The voltage and current waveforms of D_A , which vary from -24 to 0.3v and from 0 to 22.5A, are interpreted by the Diode (D_A) graph 14. These waveforms are represented by the colors blue and red. When the condition of the switches is On. The Diode's (D_B) voltage and current waveforms graph 15, which spans from 0 to 270A and -73.9 to 0.6v, are interpreted. The waveforms are represented by the colors Blue and maroon. When the switches are not in conduction mode. Waveforms of the Diode's (D_c) voltage and current graph 15, which spans from 0 to 6A and -74 to 0.3v, are interpreted. These waveforms are represented by the colors red and purple.

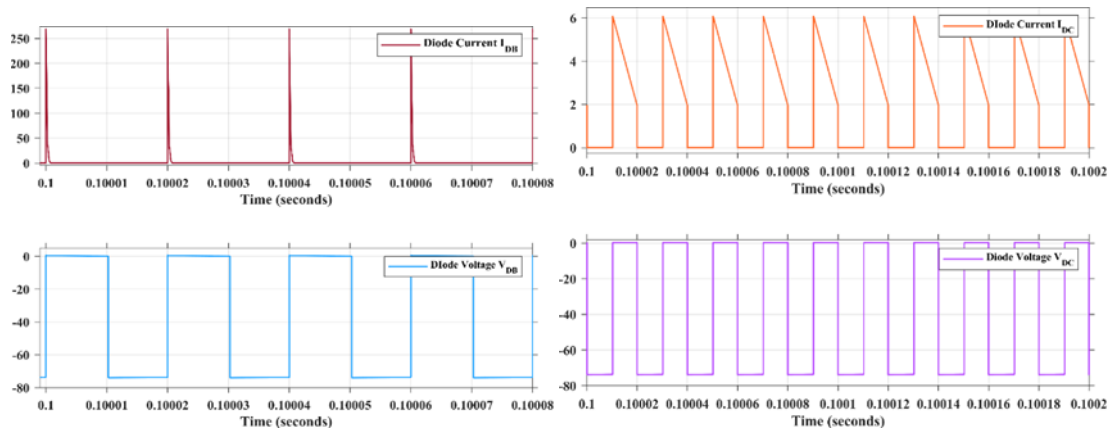


Fig 16. Voltage and Current waveforms of Diode Dc.

3.1 Comparison

REFERENCES	V_{IN} (V)	L_1 (μ H)	L_2 (μ H)	L_3 (μ H)	L_4 (μ H)	L_5 (μ H)	C_1 (μ F)	C_2 (μ F)	C_3 (μ F)	C_4 (μ F)	C_5 (μ F)	V_{OUT} (V)
[1]	12	1	490	-	-	-	100	100	100	-	-	85
[2]	30	4	-	-	-	-	50	7.5	-	-	-	180
[3]	48	680	680	-	-	-	220	10	4.7	4.7	-	360
[4]	24	307.2	307.2	-	-	-	180	180	180	27.8	-	240
[7]	20	100	560	-	-	-	100	100	100	100	100	200
[8]	40	54	54	5	20	20	10	10	30	10	-	400
[10]	20	62.24	62.32	2.1	2.2	-	4.4	4.4	220	-	-	400
PROPOSED	12	45.8	3	-	-	-	164.4	80	80	-	-	100

TABLE 2. Comparison among different DC-DC Converters.

The table 2 provides a comparative overview of different configurations. Each row represents a unique element characterized by its input voltage, inductance values, capacitance values, and resulting output voltage. Based on these findings it can be inferred that the proposed converter is used for wind applications. Unlike, the other DC-DC converters, the proposed converter offers a suitable voltage gain than alternatives.

REFERENCES	No of Inductors	No of Capacitors
[1]	2	3
[2]	1	2
[3]	2	4
[4]	2	4
[7]	2	5
[8]	5	4
[10]	4	3
PROPOSED	2	3

TABLE 3. Number of components in different DC-DC Converters.

Duty ratio	Output Voltage	Output Power	%Efficiency	Ripple factor
10%	40.22	32.35	96.54	0.05594
15%	44.73	40.01	96.61	0.11178
20%	50.04	50.1	97.04	0.119904
25%	55.8	62.3	97.2	0.14336
30%	61.96	76.83	97.32	0.16139
35%	68.5	93.9	97.4	0.18715

40%	75.35	113.6	97.44	0.176244
45%	82.69	136.9	97.47	0.2321
50%	93.85	176.3	97.91	0.24758
51.34%	97.79	191.5	97.94	0.25718
55%	110.2	243.2	98.03	0.274954
60%	132.2	350.2	98.12	0.298789
65%	163.2	533.7	98.17	0.32475
70%	208.9	874.2	98.05	0.359023
75%	281.1	1583	97.72	0.380647
80%	405.3	3292	96.62	0.399703
85%	643.5	8298	92.9	0.424553

TABLE 4. Comparison of different Duty ratio cycles with Output voltage, Output power, %Efficiency, Ripple factor in High gain DC-DC converter.

The above table 4 shows the converter behavior with different duty ratios. When the duty ratios change the mentioned parameters will vary, they are Output voltage, Output power, %Efficiency and Ripple factor. For a converter the ripple factor will be less than 1. The figs. 17 to 20 shows the plots of the values given in table 4. The table 5 represents the duty ratio cycle and frequency. The two most important factors in waveform production are frequency and duty cycle. The frequency tends to drop when we raise the duty cycle, or the amount of time the signal is higher. Converter are always required to maintain load safety since a drop in output voltage ripple % is the result of switching frequency. Additionally, output voltage ripple is rising in parallel with rising duty ratio (raising current).

REFERENCES	FREQUENCY (fs) kHz	DUTY CYCLE(D)
[1]	50	0.4
[2]	10	0.7
[3]	50	0.5
[4]	50	0.8
[7]	31.33	0.5
[8]	100	0.7
[10]	80	0.7
PROPOSED	50	0.5134

TABLE 5. Comparison of various DC-DC converters' duty ratio and frequency cycles.

References	Switches	Diodes
1	$V_{S1} = \frac{1}{(1-D)} V_i$ $V_{S1} = \frac{(2-D)}{(1-D)^2} V_i$	$V_{D1} = V_{D1} = \frac{1}{(1-D)} V_i$ $V_{D3} = V_{D0} = \frac{2}{(1-D)^2} V_i$
7	$V_{S1} = \frac{V_{in}}{(D-1)^2}$ $V_{D1} = \frac{D * V_{in}}{(D-1)^2}$	$V_{D2} = \frac{V_{in}}{(1-D)}$ $V_{D3} = V_{D4} = V_{D5} = V_{D6} = \frac{V_{in}}{(D-1)^2}$
10	$V_{S2} = V_{S1} = \frac{1}{(1-D)} V_{in}$	$V_{D0} = V_{D1} = V_{D2} = V_0 - V_{C1}$ $= \frac{2+2N}{3+3N} V_0 = \frac{2}{3} V_0$
13	$V_{S1} = \frac{V_{in}}{(1-D)} = \frac{V_0(1-D)}{(1+D-D^2)}$ $V_{S1} = \frac{V_{in}}{(1-D)^2} = \frac{V_0}{(1+D-D^2)}$	-
14	$V_{S2} = \frac{V_{in}}{(1-D)^2} = \frac{V_0}{(4-4D+D^2)}$	$V_{D1} = V_{D4} = \frac{V_{in}}{(1-D)} = \frac{V_0(1-D)}{(4-4D+D^2)}$

		$V_{D2} = \frac{2V_{in}}{(1-D)} = \frac{2V_0(1-D)}{(4-4D+D^2)}$ $V_{D3} = \frac{V_{in}(2-D)}{(1-D)} = \frac{V_0(2-D)}{(4-4D+D^2)}$
15	$V_s = \frac{V_{in}}{(1-D)^2} = \frac{V_0}{(3-D)}$	$V_{D1} = \frac{V_{in}}{(1-D)} = \frac{V_0(1-D)}{(3-D)}$ $V_{D2} = V_{D3} = V_{D4} = V_{D5} = \frac{V_{in}}{(1-D)^2} = \frac{V_0}{(3-D)}$ $V_{D6} = \frac{DV_{in}}{(1-D)^2} = \frac{DV_0}{(3-D)}$

TABLE 6. Comparison of various DC-DC converter’s Voltage stresses.

The switches and diodes in power electronics, which are commonly employed in voltage regulators and converters, are shown in the table 6 in a variety of configurations and equations. *Switches*: The voltage across switches in various configurations is represented by these equations, which are frequently described in terms of input voltage, duty cycle, and other factors like output voltage. *Diodes*: The voltage drop across diodes is described in detail by the equations, which is essential knowledge for comprehending power conversion efficiency and losses. Input voltage, duty cycle, and perhaps output voltage are also factors that affect them.

IV. CONCLUSION

To improve the output voltage capabilities of the High Gain Boost Converter, a comprehensive evaluation and analysis of its performance have been conducted. It has been repeatedly confirmed that the High gain boost converter finds applications in a wide range of renewable energy systems, even after a thorough analysis of different converters and topologies. In order to identify the best converter for wind turbines and solar panels, in-depth analyses of each converter are conducted, along with comparison research. In the context of solar panels and wind turbines, this research also explores the function, difficulties, and potential applications of DC-DC converters. It also provides a thorough analysis of each multistage converter's benefits, drawbacks, and particular uses.

REFERENCES

[1] Qusay Hassan, Sameer Algburi, Aws Zuhair Sameen, Hayder M. Salman, Marek Jaszczur, A review of hybrid renewable energy systems: Solar and wind-powered solutions: Challenges, opportunities, and policy implications, Results in Engineering, Volume 20, 2023, 101621, ISSN 2590-1230, <https://doi.org/10.1016/j.rineng.2023.101621>.

[2] TY - JOUR AU - Ahmed, Hassan AU - Abdel-Rahim, Omar AU - Ali, Ziad PY - 2022/02/26 SP - 734 T1 - New High-Gain Transformerless DC/DC Boost Converter System VL - 11 DO - 10.3390/electronics11050734 JO - Electronics ER

[3] M. Rezvanyvardom, A. Mirzaei, M. Shabani, Saad Mekhilef, Muhyaddin Rawa, Addy Wahyudie, Mahrous Ahmed, Interleaved step-up soft-switching DC–DC Boost converter without auxiliary switches, Energy Reports, Volume 8, 2022, Pages 6499-6511, ISSN 2352-4847, <https://doi.org/10.1016/j.egy.2022.04.069>.

[4] N. Subhani, Z. May, Md. K. Alam, I. Khan, M. A. Hossain, and S. Mamun, “An improved non-isolated quadratic DC–DC boost converter with ultra high gain ability,” *IEEE Access*, vol. 11, pp. 11350–11363, 2023, doi: [10.1109/ACCESS.2023.3241863](https://doi.org/10.1109/ACCESS.2023.3241863).

[5] R. V. Damodaran, H. Shareef, K. S. P. Kiranmai, and R. Errouissi, “Two-switch boost converter with improved voltage gain and degree of freedom of control,” *IEEE Access*, vol. 11, pp. 23827–23838, 2023, doi: [10.1109/ACCESS.2023.3249107](https://doi.org/10.1109/ACCESS.2023.3249107).

[6] S. Pirpoor, S. Rahimpour, M. Andi, N. Kanagaraj, S. Pirouzi, and A. H. Mohammed, “A novel and high-gain switched-capacitor and switched-inductor-based DC/DC boost converter with low input current ripple and mitigated voltage stresses,” *IEEE Access*, vol. 10, pp. 32782–32802, 2022, doi: [10.1109/ACCESS.2022.3161576](https://doi.org/10.1109/ACCESS.2022.3161576).

[7] M. A. Al-Saffar and E. H. Ismail, “A high voltage ratio and low stress DC–DC converter with reduced input current ripple for fuel cell source,” *Renew. Energy*, vol. 82, pp. 35–43, Oct. 2015, doi: [10.1016/j.renene.2014.08.020](https://doi.org/10.1016/j.renene.2014.08.020).

[8] A. Allehyani, “Analysis of a transformerless single switch high gain DC–DC converter for renewable energy systems,” *Arabian J. Sci. Eng.*, vol. 46, no. 10, pp. 9691–9702, Oct. 2021, doi: [10.1007/s13369-021-05472-3](https://doi.org/10.1007/s13369-021-05472-3).

- [9] L. Yang, W. Yu, and J. Zhang, "High voltage gain ratio isolated resonant switched-capacitor converter for sustainable energy," *IEEE Access*, vol. 7, pp. 23055–23067, 2019, doi: [10.1109/ACCESS.2019.2893981](https://doi.org/10.1109/ACCESS.2019.2893981).
- [10] J. Ahmad, M. Zaid, A. Sarwar, C.-H. Lin, M. Asim, R. K. Yadav, M. Tariq, K. Satpathi, and B. Alamri, "A new high-gain DC–DC converter with continuous input current for DC microgrid applications," *Energies*, vol. 14, no. 9, p. 2629, May 2021.
- [11] J. Ahmad, C.-H. Lin, M. Zaid, A. Sarwar, S. Ahmad, M. Sharaf, M. Zaindin, and M. Firdausi, "A new high voltage gain DC to DC converter with low voltage stress for energy storage system application," *Electronics*, vol. 9, no. 12, p. 2067, Dec. 2020.
- [12] Reddy, B. Nagi, G. Vinay Kumar, B. Vinay Kumar, B. Jhansi, B. Sandeep, and K. Sarada. "Fuel Cell Based Ultra-Voltage Gain Boost Converter for Electric Vehicle Applications." *Transactions on Energy Systems and Engineering Applications: TESEA* 4, no. 1 (2023): 68-90.
- [13] Rekha, R., Srikanth Goud, B., Rami Reddy, C., Nagi Reddy, B. (2020). PV-Wind-Integrated Hybrid Grid with P&O Optimization Technique. In: Saini, H., Srinivas, T., Vinod Kumar, D., Chandragupta Mauryan, K. (eds) *Innovations in Electrical and Electronics Engineering. Lecture Notes in Electrical Engineering*, vol 626. Springer, Singapore. https://doi.org/10.1007/978-981-15-2256-7_53.
- [14] J. Ahmad, C.-H. Lin, M. Zaid, A. Sarwar, S. Ahmad, M. Sharaf, M. Zaindin, and M. Firdausi, "A new high voltage gain DC to DC converter with low voltage stress for energy storage system application," *Electronics*, vol. 9, no. 12, p. 2067, Dec. 2020.
- [15] S. Khan, M. Zaid, A. Mahmood, J. Ahmad, and A. Alam, "A single switch high gain DC–DC converter with reduced voltage stress," in *Proc. IEEE 7th Uttar Pradesh Sect. Int. Conf. Electr., Electron. Comput. Eng. (UPCON)*, Nov. 2020, pp. 1–6.